Attaching negative structures to model cut-outs in the vibration analysis of structures

Y. Mochida[1], S. Ilanko[1*], D. Kennedy[2]

[1]The School of Engineering, The University of Waikato, New Zealand,

[2]School of Engineering, Cardiff University, United Kingdom,

[*]ilanko@waikato.ac.nz

Abstract

The presence of a hole, cut-out or void in a structure makes it difficult to be modelled for calculating natural frequencies. A theoretical basis for simplifying the modelling of cut-outs in a structure by attaching a negative structure is presented. The Dynamic Stiffness Method has been used to prove that this method yields the required natural frequencies. The derivations also show the presence of additional natural frequencies which correspond to the vibration of the positive and negative parts vibrating together while the actual structure with the hole or cut-out usually remains stationary.

1. Introduction

Determination of natural frequencies, critical loads and stress distribution in solid bodies with voids, holes, cut-outs or damages is increasingly becoming important in applications such as optimisation and damage detection [1-6]. The natural frequencies of such systems are commonly obtained using the Finite Element Method (FEM) [7-16]. There have also been some papers [17-19] which use analytical procedures such as the Rayleigh-Ritz Method (RRM) [20-22] in which the potential and kinetic energy terms of the structure are found by subtracting the energy terms associated with the void part from that of the larger structure (without the void), by taking the displacement forms of the void to be the same as those of the larger structure. In one recent approach [23], called the Independent Coordinate Coupling Method (ICCM), the displacement forms of the void and the larger domain are constrained to have similar values using Lagrangian type constraints in an average integral form. This method has been generalized in [24] which deals with the modeling of plate-like structures with holes as a basis for a structural optimization process. Once the coupling is done, the energy terms corresponding to the void are subtracted from that of the larger structure and the Rayleigh-Ritz minimisation is then carried out.

This work stems from the authors' attempts to investigate the possibility of using the modes of both the structure without any void and a negative structure corresponding to the void and then combining the two sets of modes while enforcing the embedding continuity conditions by the penalty method [25, 26] or the Lagrangian Multiplier Method (LMM) [27] in a Rayleigh-Ritz procedure. Numerical experimentation with this idea using discrete systems, beams and plates with cut-outs and holes showed that while it is possible to obtain the required frequencies, the presence of additional natural frequencies and the difficulty in

choosing appropriate shape functions and constraint enforcement methods pose some challenges [28]. Thus the authors proceeded to study the theoretical basis for combining positive and negative structures, using the Dynamic Stiffness Method (DSM), the derivations and findings of which are presented in this paper, along with some numerical results. The paper shows that the required natural frequencies are obtainable from the model incorporating a negative structure, and explains the additional frequencies.

2. The theoretical basis

2.1 Existence of natural frequencies of the structure with a hole in the proposed model

In order to develop a theoretical framework, the question will first be addressed of whether or not all the required natural frequencies and modes of at least a certain class of structures containing voids can be obtained through the proposed method. The hypothesis taken is that these characteristics are obtainable by combining the modes of positive and negative structures, i.e. by embedding a negative structure with known modes into a larger positive structure with known modes, and analysing the combined system.
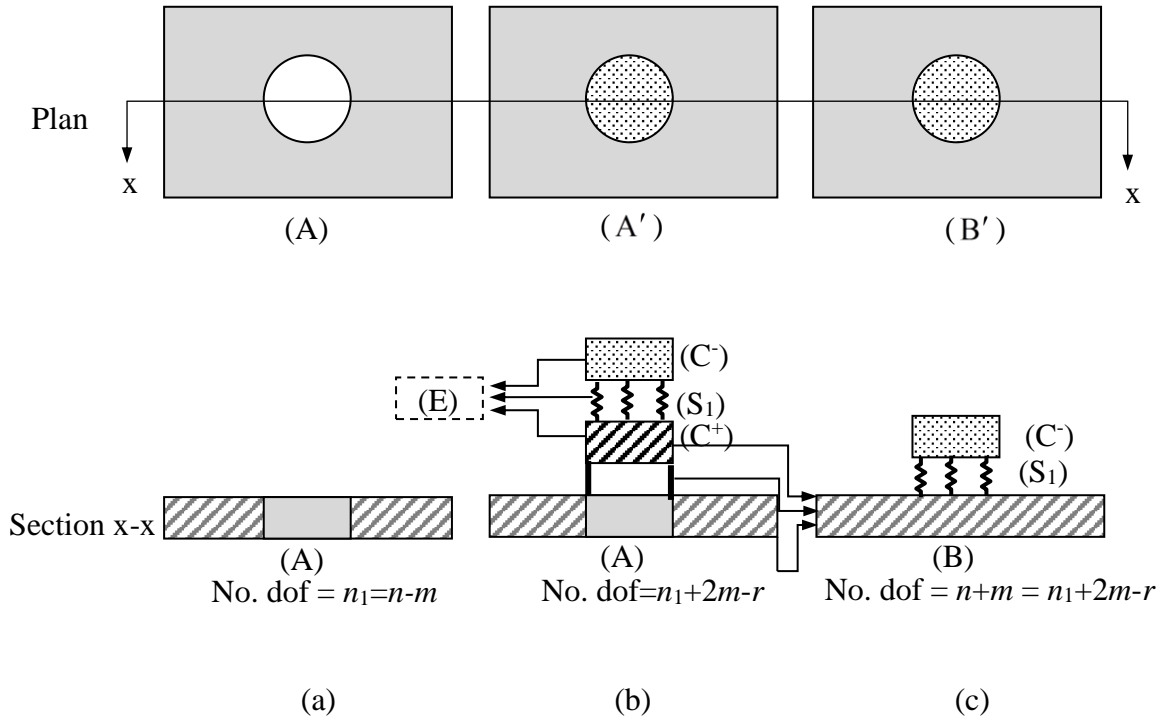

Fig. 1 Example of plates combining positive and negative structures

Consider the case of a structure A which contains a hole, represented in Fig. 1a by a rectangular plate with a circular hole. Now consider two elastic structural bodies C^+ and C^-, having identical shapes that would fill the void in A, one (C^+) with the same distribution of elastic and inertial properties as that of A, and the other (C^-) with negative properties but of the same magnitude. In this case C^+ and C^- will be circular plates. Then consider joining C^+ and C^- by means of a very stiff elastic continuum S_1, which acts as a penalty against any differential displacement between the two elements. The resulting structure has the potential to exist as an empty element (E). The term 'empty' is used here to indicate that the element could be subjected to any dynamic displacement without inducing any forces (or moments) at the boundaries. This empty element state occurs only in modes in which C^+ and C^- vibrate together with the same displacement. The combined unit, being empty, would not change the behaviour of any structure to which it is attached as there will not be any unbalanced forces or moments. This combined unit is now connected to Structure A along the common boundary with the hole (in this case having a circular circumference), by constraining the degrees of freedom to be the same. This may be done either by using a penalty parameter or by using sufficiently large number (say r) of discrete constraints. It may be seen that the resulting structure A′ (see Fig. 1b) is capable of possessing all the natural frequencies and modes of A, because it was formed just by the addition of the empty element E. Furthermore, if the penalty stiffness is sufficiently large, from the asymptotic modelling theorems [29], the combination of A and C^+ is equivalent to B (the rectangular plate without any hole). Connecting B to C^- using S_1 gives B′ as shown in Fig. 1c. It is therefore deduced that the natural frequencies and modes of B′ would include those of A. The hole in a plate is only an illustration but the same argument will hold for a body with cut-outs or voids. This will be proved formally for discrete systems in the next section.

2.2 Proof of existence of the required natural frequencies for discrete systems

Consider a discrete structural system A (Fig. 2a) having n_1 vibratory degrees of freedom which is obtainable from a larger system B (Fig. 2b) by removing some elements. A represents the structure with a cut-out and B is a larger structure which would be the result of filling the cut-out part. For simplicity, the discrete systems are represented with spring-mass arrangements. The proposed method involves attaching a negative structure C^- (Fig. 2c) to the larger positive structure B to obtain B′ as illustrated in Fig. 2d. Thus C^- would potentially cancel the stiffness and inertia in a part of A so as to produce A if it is rigidly connected to its positive counterpart within B. The masses associated with the degrees of freedom of A are

shown as lightly filled circles and rectangles. The circles correspond to the internal degrees of freedom that do not lie on the common boundary with the hollow domain while the rectangles correspond to degrees of freedom that are on the boundary. The set of internal degrees of freedom of A will be denoted by vector $\mathbf{q_{Ai}}$ and the common degrees of freedom will be denoted by $\mathbf{q_e}$. Let the natural frequencies of A be $\boldsymbol{\omega_A}$, a vector set containing $\omega_{A,1}, \omega_{A,2}, .. \omega_{A,n1}$. Now consider another discrete system C^+ (Fig. 2e) with m vibratory degrees of freedom which is the positive counterpart of C^- and represents the component of B if it did not have the cut-out. This means System C^- has the same magnitude of stiffness and inertial properties as C^+ but with opposite sign. The masses associated with the positive structure are shown as black circles or squares and their negative counterparts are shown as white circles and squares with dotted boundaries. Now consider linking these to system A at a common boundary where the masses associated with the shared degrees of freedom $\mathbf{q_e}$ are shown in squares. The circles depict the masses that are not associated with a common boundary with A (i.e. at internal degrees of freedom). These sets of internal degrees of freedom of C^+ and C^- are labelled $\mathbf{q_{Pi}}$ and $\mathbf{q_{Ni}}$ respectively, to indicate the internal degrees of freedom of the positive and negative structures. The natural frequencies of C^+ are $\boldsymbol{\omega_C} = [\omega_{C,1}, \omega_{C,2}, .. \omega_{C,m}]$. As both inertial and elastic (stiffness) properties of C^- are equal and opposite to those of C^+, each term in the equation of motion of C^- would be equal and opposite to the corresponding term for C^+. This means the natural frequencies and modes of C^- are identical to those of C^+. For the purpose of this proof, it is necessary to consider System A' shown in Fig. 2f, which is formed by joining A, C^+ and C^- rigidly at the common boundary (i.e. the degrees of freedom at the boundary between the three systems are common for them) and joining other corresponding degrees of freedom between C^+ and C^- by means of elastic springs S_1.

As the connection between A and C+ in A' is rigid,

$$A' \equiv B' \tag{1}$$
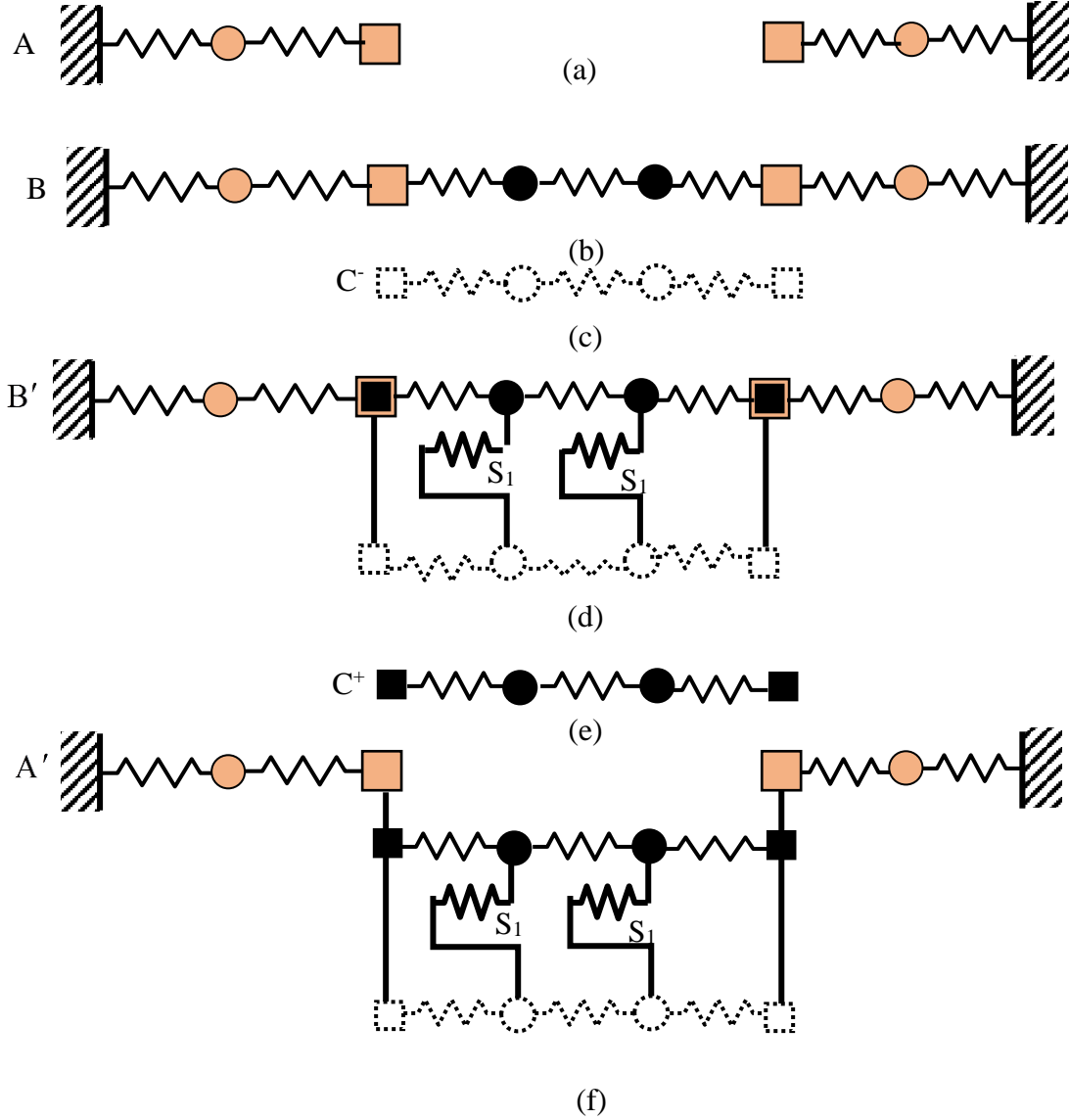
Fig. 2 Spring-mass systems representing embedded negative structures

In order to justify the use of a system with embedded/tied negative structure representing a structure with a void/hole/cut-out, it will be shown that:

The eigensolution of system A is also an eigensolution of system B'.   Statement (a)

In the modes of the above eigensolution, positive and negative structures C^+ and C^- vibrate together, while A vibrates in one of its natural modes.   Statement (b)

It will also be shown that this model will produce additional natural frequencies and modes, and that in general these extra modes do not involve vibration of the actual structure A which will remain stationary. The only exceptions are cases where such spurious modes also share the same eigenvalues as those of A.

<u>Proof:</u>

The eigenvalue equation for A' may be written as:

$$
\begin{pmatrix}
\mathbf{K}_{Cii} + \mathbf{K}_{S1i} & -\mathbf{K}_{S1i} & \mathbf{0} & \mathbf{K}_{Cie} \\
-\mathbf{K}_{S1i} & -\mathbf{K}_{Cii} + \mathbf{K}_{S1i} & \mathbf{0} & -\mathbf{K}_{Cie} \\
\mathbf{0} & \mathbf{0} & \mathbf{K}_{Aii} & \mathbf{K}_{Aie} \\
\mathbf{K}_{Cei} & -\mathbf{K}_{Cei} & \mathbf{K}_{Aei} & \mathbf{K}_{Aee}
\end{pmatrix}
\begin{pmatrix}
\mathbf{q}_{Pi} \\
\mathbf{q}_{Ni} \\
\mathbf{q}_{Ai} \\
\mathbf{q}_{e}
\end{pmatrix} =
$$

$$
\omega^2
\begin{pmatrix}
\mathbf{M}_{Cii} & \mathbf{0} & \mathbf{0} & \mathbf{M}_{Cie} \\
\mathbf{0} & -\mathbf{M}_{Cii} & \mathbf{0} & -\mathbf{M}_{Cie} \\
\mathbf{0} & \mathbf{0} & \mathbf{M}_{Aii} & \mathbf{M}_{Aie} \\
\mathbf{M}_{Cei} & -\mathbf{M}_{Cei} & \mathbf{M}_{Aei} & \mathbf{M}_{Aee}
\end{pmatrix}
\begin{pmatrix}
\mathbf{q}_{Pi} \\
\mathbf{q}_{Ni} \\
\mathbf{q}_{Ai} \\
\mathbf{q}_{e}
\end{pmatrix}
\tag{2}
$$

Combining the stiffness and mass terms this may be written as:

$$
\begin{pmatrix}
\mathbf{K}^*_{Cii} + \mathbf{K}_{S1i} & -\mathbf{K}_{S1i} & \mathbf{0} & \mathbf{K}^*_{Cie} \\
-\mathbf{K}_{S1i} & -\mathbf{K}^*_{Cii} + \mathbf{K}_{S1i} & \mathbf{0} & -\mathbf{K}^*_{Cie} \\
\mathbf{0} & \mathbf{0} & \mathbf{K}^*_{Aii} & \mathbf{K}^*_{Aie} \\
\mathbf{K}^*_{Cei} & -\mathbf{K}^*_{Cei} & \mathbf{K}^*_{Aei} & \mathbf{K}^*_{Aee}
\end{pmatrix}
\begin{pmatrix}
\mathbf{q}_{Pi} \\
\mathbf{q}_{Ni} \\
\mathbf{q}_{Ai} \\
\mathbf{q}_{e}
\end{pmatrix} = \mathbf{0}
\tag{3}
$$

where

$$
\mathbf{K}^*_{Cii} = \mathbf{K}_{Cii} - \omega^2 \mathbf{M}_{Cii}, \quad \mathbf{K}^*_{Cie} = \mathbf{K}_{Cie} - \omega^2 \mathbf{M}_{Cie}, \quad \mathbf{K}^*_{Cei} = \mathbf{K}_{Cei} - \omega^2 \mathbf{M}_{Cei} = (\mathbf{K}^*_{Cie})^T,
$$

$$
\mathbf{K}^*_{Aii} = \mathbf{K}_{Aii} - \omega^2 \mathbf{M}_{Aii}, \quad \mathbf{K}^*_{Aie} = \mathbf{K}_{Aie} - \omega^2 \mathbf{M}_{Aie}, \quad \mathbf{K}^*_{Aei} = \mathbf{K}_{Aei} - \omega^2 \mathbf{M}_{Aei} = (\mathbf{K}^*_{Aie})^T,
$$

$$
\mathbf{K}^*_{Aee} = \mathbf{K}_{Aee} - \omega^2 \mathbf{M}_{Aee},
$$

Equation (3) can be expressed in terms of the vectors $\mathbf{u}_i = (\mathbf{q}_{Pi} + \mathbf{q}_{Ni})/2$ and $\mathbf{v}_i = (\mathbf{q}_{Pi} - \mathbf{q}_{Ni})/2$ as

$$
\begin{pmatrix}
2\mathbf{K}^*_{Cii} & 4\mathbf{K}_{S1i} & \mathbf{0} & 2\mathbf{K}^*_{Cie} \\
\mathbf{0} & 2\mathbf{K}^*_{Cii} & \mathbf{0} & \mathbf{0} \\
\mathbf{0} & \mathbf{0} & \mathbf{K}^*_{Aii} & \mathbf{K}^*_{Aie} \\
\mathbf{0} & 2\mathbf{K}^*_{Cei} & \mathbf{K}^*_{Aei} & \mathbf{K}^*_{Aee}
\end{pmatrix}
\begin{pmatrix}
\mathbf{u}_i \\
\mathbf{v}_i \\
\mathbf{q}_{Ai} \\
\mathbf{q}_{e}
\end{pmatrix} = \mathbf{0}
\tag{4}
$$

The determinantal eigenvalue equation of the matrix in Eq. (4) is

$$
(|2\mathbf{K}^*_{Cii}|)^2
\begin{vmatrix}
\mathbf{K}^*_{Aii} & \mathbf{K}^*_{Aie} \\
\mathbf{K}^*_{Aei} & \mathbf{K}^*_{Aee}
\end{vmatrix} = 0
\tag{5}
$$

So the eigenvalues are given by one of the two following cases.

Case (1)

$$\begin{vmatrix} \mathbf{K}^*_{Aii} & \mathbf{K}^*_{Aie} \\ \mathbf{K}^*_{Aei} & \mathbf{K}^*_{Aee} \end{vmatrix} = 0 \text{ , i.e. those of structure A,} \tag{6a}$$

Noting that the combination of $\mathbf{q}_{Ai}$ and $\mathbf{q}_e$ results in the full set of degrees of freedom of Structure A ($\mathbf{q}_A$) it may be seen that the eigenvalues are therefore the eigenvalues of A, with the boundary between A and C being unconstrained.

When Eq. (6a) is satisfied,

$$\begin{bmatrix} \mathbf{K}^*_{Aii} & \mathbf{K}^*_{Aie} \\ \mathbf{K}^*_{Aei} & \mathbf{K}^*_{Aee} \end{bmatrix} \begin{pmatrix} \mathbf{q}_{Ai} \\ \mathbf{q}_e \end{pmatrix} = \begin{pmatrix} \mathbf{0} \\ \mathbf{0} \end{pmatrix} \tag{6b}$$

Thus the natural frequencies and modes of A are a subset of the natural frequencies and modes of A'. i.e.

$$\omega_A \subset \omega_{A'}. \tag{7}$$

From Eq. (1),

$$\omega_A \subset \omega_{B'}. \tag{8}$$

This proves Statement (a)

The modes of this case for the domain of structure A obviously correspond to the natural modes of A. It is interesting to investigate what happens to the components C^+ and C^-

Substituting the second row of Eq. (6b) into the fourth row of Eq. (4) gives $\mathbf{K}^*_{Cei}\mathbf{v}_i = \mathbf{0.}$

This implies that $\mathbf{v}_i = \mathbf{0}$, so that $\mathbf{q}_{Pi}$ and $\mathbf{q}_{Ni}$ are equal and the constraints between the positive structure and its negative counterpart, C^- are fulfilled.

Thus the positive and negative structures C^+ and C^- vibrate together which proves Statement (b).

This is understandable as the net energy from the vibration of the positive and negative components will be zero and there will not be any residual stress at the boundary between A and C making it an unconstrained boundary for A. This case accounts for n_1 modes.

Case (2)

The second scenario for Eq. (5) is

$$|2\mathbf{K}^*_{Cii}| = 0 \tag{9a}$$

This root has a multiplicity of 2 and corresponds to the structures C$^+$ and C$^-$, but with the boundary between A and C being fixed (this is because the only degrees of freedom included are internal ones).

Thus Eq. (9a) is associated with the following equations

$$\mathbf{K}^*_{Cii}\mathbf{q}_{Pi} = \mathbf{K}^*_{Cii}\mathbf{q}_{Ni} = \mathbf{0} \tag{9b}$$

$$\mathbf{q}_e = \mathbf{0} \tag{9c}$$

This case offers 2(m-r) eigenvalues.

From Eq. (9c) and the third row of Eq. (4), $\mathbf{K}^*_{Aii}\mathbf{q}_{Ai} = \mathbf{0}$, which may be satisfied in two ways.

Case (2a)

$$\mathbf{q}_{Ai} = \mathbf{0} \tag{10a}$$

Case (2b)

$$|\mathbf{K}^*_{Aii}| = 0 \tag{10b}$$

Case (2b) implies that the solution also corresponds to the eigensolution for Structure A when its boundary with C is fully constrained. Thus, the eigenvalues of A with the boundary constrained must coincide with the eigenvalues of Structures C$^+$ and C$^-$, also with their boundaries clamped. This can be treated as a special case, the more likely scenario being Case (2a). For Case (2a), from Eqs (10a) and (9c), none of the degrees of freedom of A would participate in the vibration. Structures C$^+$ and C$^-$ with their boundaries with A fully constrained, will vibrate in their natural modes. For this case, consider the first row of Eq. (4).

$$2\mathbf{K}^*_{Cii}\mathbf{u}_i + 4\mathbf{K}_{S1i}\mathbf{v}_i + 2\mathbf{K}^*_{Cei}\mathbf{q}_e = \mathbf{0}$$

From Eqs (9b) and (9c) it may be seen that the first and third terms of the above equation are zero, so that $\mathbf{K}_{S1i}\mathbf{v}_i = \mathbf{0}$.

If C$^+$ and C$^-$ are connected by elements that provide non-zero stiffness (i.e. if $\mathbf{K}_{S1i} \neq \mathbf{0}$) then $\mathbf{v}_i = \mathbf{0}$. This means that, as for Case (1), C$^+$ and C$^-$ vibrate together.

Once again, the vibration of C$^+$ and C$^-$ with the same displacements at corresponding degrees of freedom does not result in any residual stress at the boundary between A and C. However, if there are no connections between their internal degrees of freedom, these degrees of freedom may have different magnitude of displacements.

Although the above derivations were based on connected discrete systems, they hold for continuous systems consisting of skeletal frame members too as long as the connections

between the individual systems are made at a discrete number of points. The stiffness matrices $\mathbf{K}_{Cii}^*$, $\mathbf{K}_{Cie}^*$, $\mathbf{K}_{Cei}^*$, $\mathbf{K}_{Aii}^*$, $\mathbf{K}_{Aie}^*$, $\mathbf{K}_{Aei}^*$, $\mathbf{K}_{Aee}^*$ would then represent the exact dynamic stiffness matrices of the continuous systems, which take into account the distribution of mass. Such matrices are readily available for skeletal structural elements [30] and certain types of plates and shell structures. For the sake of this proof, it is not necessary to have a knowledge of the stiffness coefficients, but the existence of such a frequency dependent stiffness coefficient relating the action (force or a moment) required at a given point in a structure to produce a unit displacement (translation or rotation) at the same or a different point on the structure is sufficient. This is true irrespective of the number of connecting points. As the number of points increases towards infinity, the negative structure C⁻ would be rigidly connected to B almost everywhere on their common boundary between the negative structure and the remaining structure A. It is useful to note that the common boundary is the boundary between the structure with the void A and the negative structure and does not include the connection between the positive and negative parts that cancel each other. This means that the natural frequencies of a structure A that contains a void or hole or cut-out would be a subset of the natural frequencies of the corresponding structure without the void B when it is rigidly connected to a negative structure with the same magnitude of elastic and inertial properties along the common boundary.

In practice, the rigid connections between A and C⁻ can be enforced by using the penalty method. Thus it may be possible to use the penalty method in conjunction with the DSM for using this approach. However, generally for problems where a DSM formulation is not available, a numerical method such as the Rayleigh-Ritz Method could be applied. The results found indicate that while the method works with the Rayleigh-Ritz scheme, care should be taken to include a sufficient number of admissible functions to represent the vibration modes of the positive and negative structures and to enable the two parts to cancel each other.

3. Illustrative Examples and Discussion

A set of numerical experiments were carried out in order to investigate whether or not the above proof holds for vibration analysis of beams. First consider a beam which is split into three segments of length of l_i ($i = 1,2,3$). The beam has the total length L, Young's modulus E, second moment of area I and mass per unit length ρ, as shown in Fig. 3a. The natural frequencies are obtained by solving the eigenvalue equation using the DSM (the dynamic

stiffness matrix used is given in Appendix A) and RRM. The following admissible functions are used for the RRM with very high stiffness translational and rotational springs of very high stiffness to enforce the clamped condition as explained in [31, 32].

$$v(x) = \sum_{j=1}^{\hat{j}} a_j \phi_j(x) \tag{11a}$$

$$\phi_j(x) = \left(\frac{x}{L}\right)^{j-1} \quad (j = 1,2,3) \tag{11b}$$

$$\phi_j(x) = \cos\left(\frac{(j-3)\pi x}{L}\right) \quad (j > 4) \tag{11c}$$

where v is the lateral displacement and x is the axial coordinate along the beam and $\hat{j}$ is the number of admissible functions.

The shaded beam and white beam depict positive and negative structures respectively. The negative component has the same magnitude of stiffness and mass as those of the positive counterpart. They are connected sharing a common boundary at the joints in the DSM model, or using springs of high stiffness or Lagrangian constraints in the RRM model. Effectively this results in two independent cantilevers (Fig. 3b).
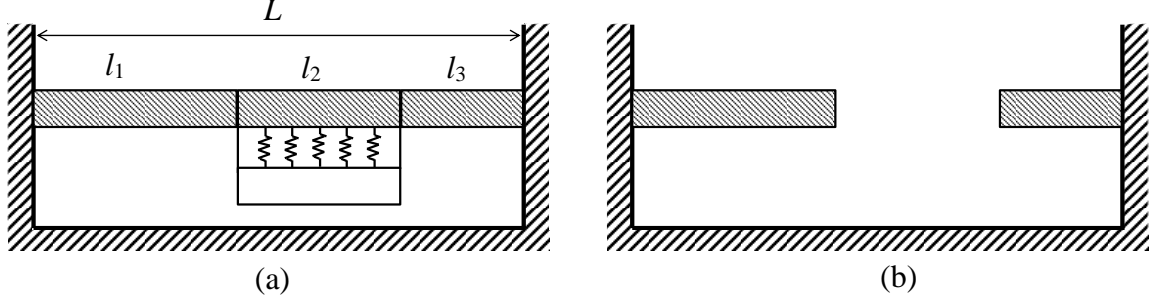

Fig 3. (a) A beam with a negative part, (b) the resultant structure

Table 1 shows the natural frequency parameters of the original structure for the first six modes for four cases where: (i) the positive and negative beams share the common boundary (at the two joints) and are connected with internal spring connection, (ii) the two beams share the common boundary only but have no internal connections, (iii) the negative beam is connected using the positive penalty springs and (iv) using Lagrangian constraints. The results for Cases (i) and (ii) are obtained using the DSM and the results for Cases (iii) and (iv) are obtained using the RRM with $\hat{j}$ =250, which is sufficient to obtain a result converged to five significant figures [31]. As can been seen from Table 1, the natural frequency parameters

for the cases (i) and (ii) are identical. This illustrates that the natural frequencies of the original structure can be obtained without the internal connection between the positive and negative beams as predicted by Statement (a). This means enforcement of rigid connections only at the boundary nodes with the negative beam is sufficient. The results for cases (iii) and (iv) have a good agreement with cases (i) and (ii). However, the RRM requires a sufficient number of internal connections to ensure that the negative part and its positive counterpart cancel each other. Convergence tests showed that 125 constraints with penalty stiffness of magnitude that is 10^{11} times the elastic stiffness are sufficient to obtain converged results to the five significant figures.

Table 1 The natural frequency parameter of the original structure,
$\Omega = l_i \sqrt[4]{\omega^2 \rho / EI}$, where l is the length of the resultant cantilever beam

Mode	Ω			
	(i)	(ii)	(iii)	(iv)
1	1.8751	1.8751	1.8751	1.8751
2	4.6941	4.6941	4.6941	4.6941
3	7.8548	7.8548	7.8547	7.8548
4	10.996	10.996	10.995	10.996
5	14.137	14.137	14.137	14.138
6	17.279	17.279	17.279	17.279

Figure 4 shows the first (top row), second (middle row) and third (bottom row) modes of these two cantilever segments, which correspond to the first three modes of the non-dimensional frequency parameters given in Table 1 respectively. Those on the left side of the figure are for the left segment and those on the right side are for the right segment. They have different lengths and so different natural frequencies, however, they have the same non-dimensionalised frequency parameters for the same modes. The horizontal axis is the axial coordinate and the vertical axis is the displacement of beams. The solid thick lines depict the mode shapes of the resultant systems and the circles and thin line depict the negative structure and the associated positive counterpart respectively, which give in sum the void system. As the figure shows, when the original structure vibrates with its natural modes the negative part and its positive counterpart vibrate together in accordance with Statement (b).
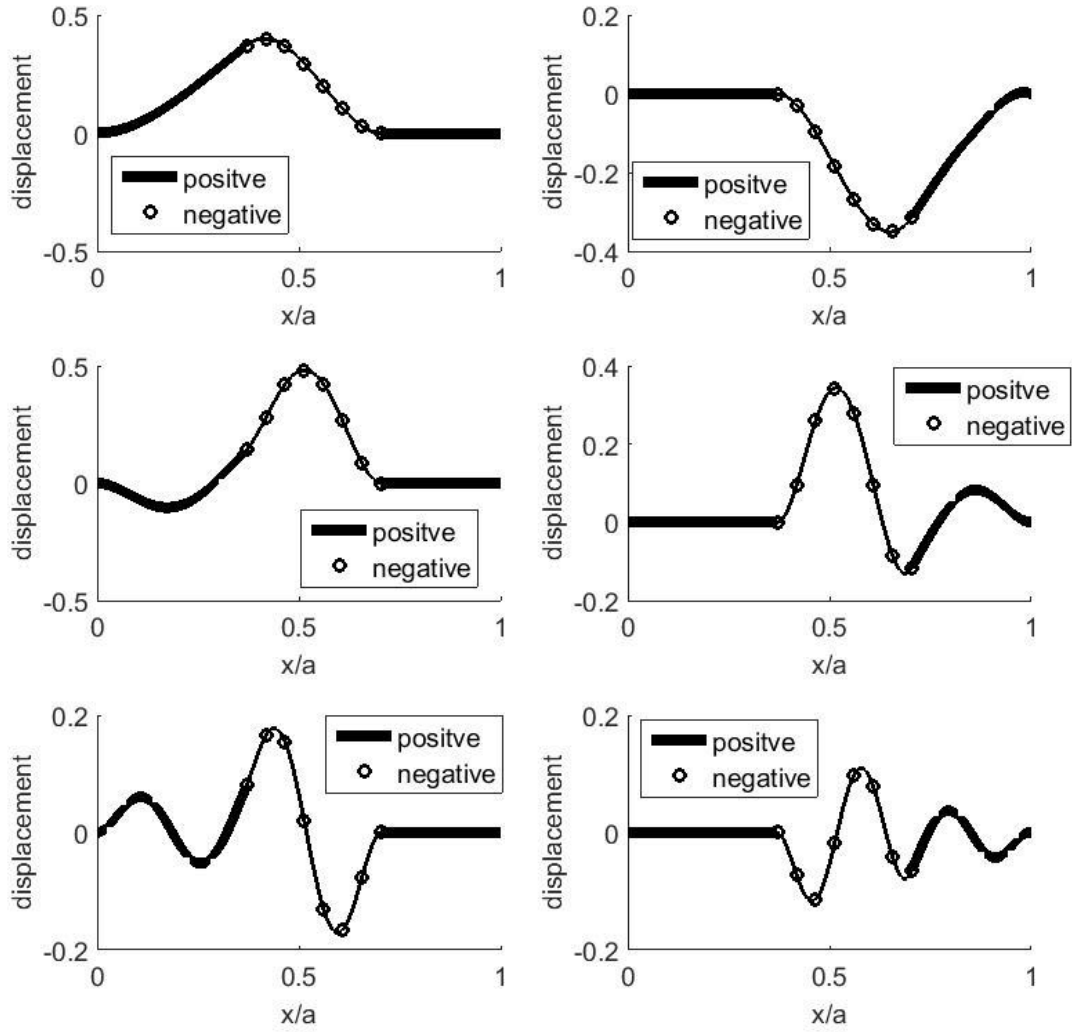
Fig. 4 First three pairs of natural modes of the cantilever beam segments.

Fig. 5 shows the spurious modes corresponding to Case (2a), obtained using the RRM with penalty springs, where the negative structure and its positive counterpart vibrate together without any violation of constraints. As can been seen from the figure, the empty structure with fixed ends vibrates while the remaining structure stays stationary including at the common nodes, as predicted in Eq. (10a), in the proof for Case (2).
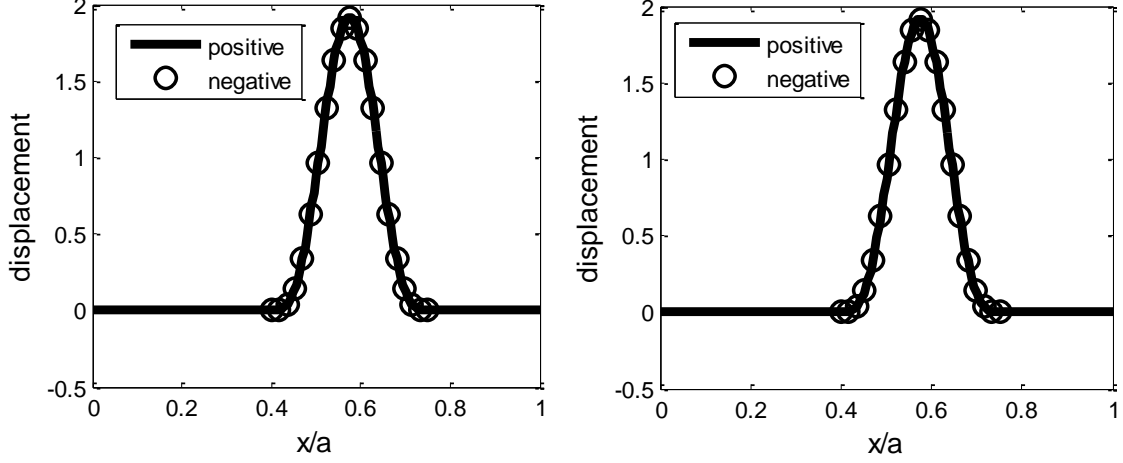
Fig. 5 Spurious modes corresponding to Case (2a).

For validation purposes, consider also the case where the positive component and the negative component are connected using Lagrangian constraints. The natural frequencies obtained using the penalty method and Lagrangian Multiplier Method agree with each other (Table 1). Using Lagrangian constraints with RRM gives the same spurious modes as ones using the penalty springs.

It is interesting to mention here the Independent Coordinate Coupling Method (ICCM), introduced by Kwak and Han [23]. In the ICCM Method, the energy of the hollow part of a structure is effectively subtracted from the energy of a larger structure. Although the positive and negative structures are not treated as independent as in the RRM with embedded or attached negative structure, the ICCM could also be considered a negative structures approach, except that the choice of admissible functions is made before the minimisation. For this reason, it was decided to recalculate the natural frequencies and modes using the ICCM. The results confirmed the published results, thus showing that the natural frequencies of the beam with the hole can be obtained. As predicted in the derivations presented here, additional modes where only the hollow part showed some displacements were also observed. It was easy to eliminate these due to non-participation of the actual beam.

The second case considered is the vibration of an unconstrained rectangular plate with a rectangular hole (see Fig. 6). Unlike beams, exact solutions for rectangular plates are available only for plates with at least one set of opposite edges with simply supported or slip-shear boundary conditions. Thus the analysis uses a combination of the Rayleigh-Ritz Method (for the positive plate) and the Finite Element method (for the negative plate). The

basic equations needed to formulate the eigenvalue equations are given in Appendix B and are taken from references [33-38]. The positive and negative plates have been connected using the Penalty Method. Detailed energy formulations for the positive and negative plates are available in [33]. The stiffness and mass matrices for the negative plate are equal and opposite to those of a positive plate with the same magnitude of elastic modulus and density.

Hole modelled by attaching a negative plate modelled by finite elements
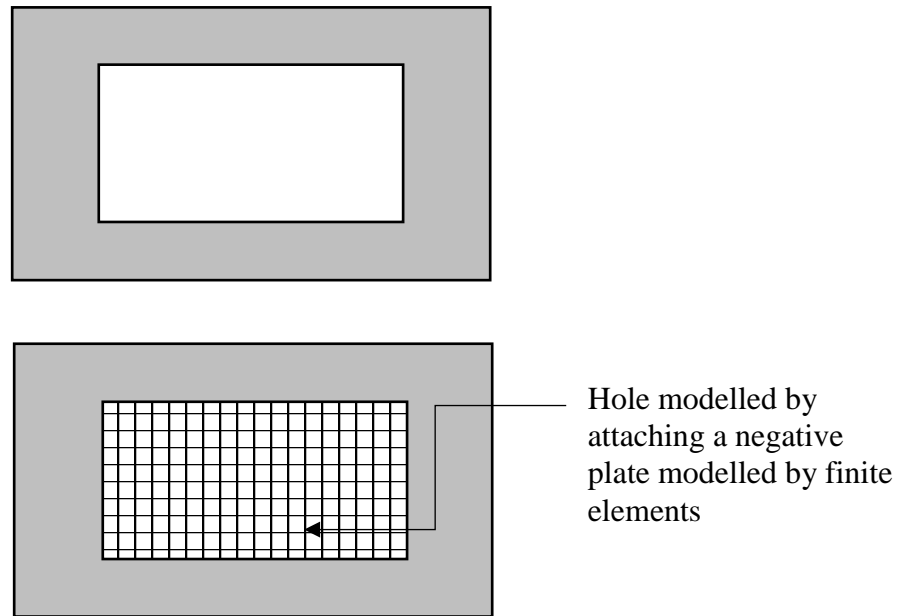
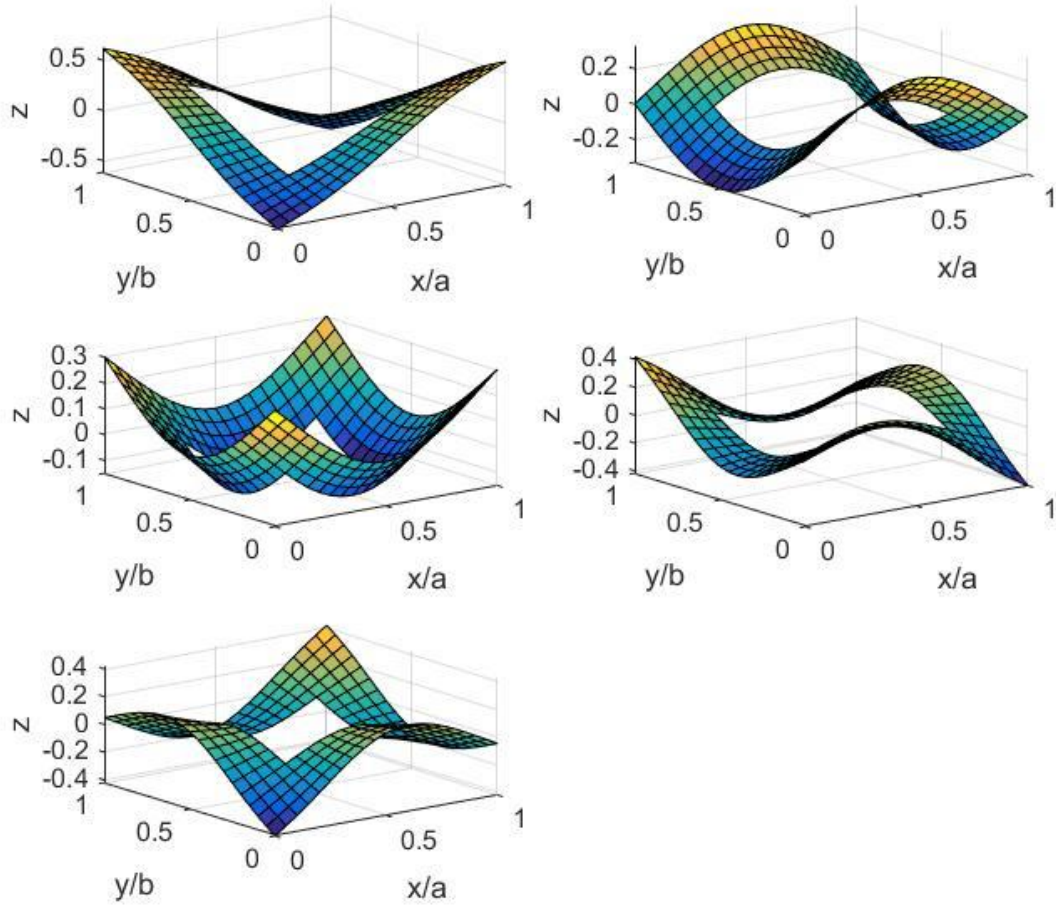Fig. 6. An unconstrained rectangular plate with a rectangular hole

Fig. 7 The first five bending modes of a completely free square plate with a square hole at the centre.

The first five non-zero modes of the plate are shown in Fig. 7. The variation of natural frequencies of the plate with N_R, the number of admissible functions (in each Cartesian coordinate direction) employed in the Rayleigh-Ritz Method, and N_F, the number of degrees of freedom in the finite element model of the negative plate, will be presented.

Table 2 gives the non-dimensional frequency parameter Ω defined by $\Omega = \omega a^2 \sqrt{\rho h / D}$. The natural frequency parameters were obtained with 20 Rayleigh-Ritz terms ($N_R = 20$) and 400 Finite Elements ($N_F = 1323$). As the plate is completely free, the first three natural frequencies are zero corresponding to the rigid-body modes. The first 5 non-zero frequency parameters give results which agree with the FEM results obtained with 972 elements (3220 dof) to 3 significant figures.

Table 2. Natural frequency parameters Ω of first five bending modes.

	Mode				
	1st	2nd	3rd	4th	5th
(1) RRM (+) and FEM (-)	10.64	15.22	22.27	31.54	31.54
(2) FEM only	10.63	15.20	22.25	31.48	31.48

It may be noted that just with the first 100 Rayleigh-Ritz modes and 1323 dof in the FEM model, the first 5 non-zero frequencies agree within 2% of the converged results. Table 3 shows the number of degrees of freedom required to obtain frequency parameters within 2% of the converged results for the first five non-rigid body modes. This is achieved with 1423 number of degrees of freedom, of which 100 degrees of freedom (number of modes) are for the larger positive plate, and 1323 dof are for the FE representation of the negative plate. Therefore, the use of a negative structure for the hollow part, represented by an FEM model, together with the first few modes of the positive plate offers a way of calculating natural frequencies and modes of a plate with a hole.

Table 3. The effect of the number of the Rayleigh-Rtiz modes on natural frequency parameters Ω (with 400 elements, (1323 dof) for the negative plate).

FEM (3220 dof)	Present (No. of modes)					
	10	20	40	60	80	100
10.63	11.13 (4.74 %)	10.88 (2.39%)	10.82 (1.83 %)	10.78 (1.45 %)	10.75 (1.17 %)	10.73 (0.98 %)
15.20	15.48 (1.88 %)	15.37 (1.15 %)	15.29 (0.63 %)	15.28 (0.56 %)	15.26 (0.43 %)	15.26 (0.43 %)
22.25	24.87 (11.8 %)	23.03 (3.52 %)	22.76 (2.31 %)	22.65 (1.81 %)	22.57 (1.45 %)	22.51 (1.18 %)
31.48	32.89 (4.48 %)	32.65 (3.72 %)	32.23 (2.38 %)	32.03 (1.75 %)	31.96 (1.52 %)	31.90 (1.33 %)
31.48	32.89 (4.48 %)	32.65 (3.72 %)	32.23 (2.38 %)	32.03 (1.75 %)	31.96 (1.52 %)	31.90 (1.33 %)

4. **Conclusions**

Using the Dynamic Stiffness Method, it has been shown that all the natural frequencies and modes of a structure (A) which contains a cut-out, hole or void are contained in the natural frequencies and modes of a larger structure attached to a negative structure (C⁻) which has equal and opposite stiffness and inertial properties of a part of the larger structure (B), which occupies the space of the cut-out, hole or void, provided that all degrees of freedom at the boundary between the positive structure and the actual structure (A) are constrained to be equal to those of the negative structure (C⁻). It has also been shown the positive and negative combined model also produces additional modes in which the corresponding positive and negative parts vibrate together at the natural frequencies of the negative structure when its boundary with the positive structure is fully constrained, while the actual structure remains stationary. It was found that there is no need to enforce continuity of displacements between the positive and negative structure except at the boundaries.

The above predictions have been demonstrated through two examples by calculating the natural frequencies and modes of: (a) a system of two cantilevers which was modelled by attaching a negative mid segment to a clamped-clamped beam; (b) a square plate with a square hole by attaching a small negative square plate in a larger positive plate. The plate problem was solved using a combination of the Rayleigh-Ritz Method and the Finite Element Method. When applying the method in a Rayleigh-Ritz scheme, while it was possible to obtain the natural frequencies and modes of the required structure with a cut-out, it was found to be necessary to enforce continuity between the positive and negative structural elements throughout the domain of the negative structure, not just at the boundaries. Further work is needed to determine the reasons. It was found that the Rayleigh-Ritz model had to be built carefully, by determining suitable penalty parameters for enforcing continuity of displacement between positive and negative structures, and the number and shapes of admissible functions.

5. **Acknowledgement**

6. References

[1] Spelsberg-Korspeter G, Wagner A. 2011, Discretization of structures using a negative stiffness approach in the context of structural optimization, *Proceedings of the 8th International Symposium on Vibrations of Continuous Systems*, Whistler, Canada.

[2] Wagner A, Spelsberg-Korspeter G, Hagedorn P. 2014, Structural optimization of an asymmetric brake disc with cooling channels to avoid squeal, *Journal of Sound and Vibration*, 333, 1888-1898.

[3] Spelsberg-Korspeter G. 2010, Structural optimization for the avoidance of self-excited vibrations based on analytical models, *Journal of Sound and Vibration*, 329, 4829–4840.

[4] Spelsberg-Korspeter G. 2009, Breaking of symmetries for stabilization of rotating continua in frictional contact, *Journal of Sound and Vibration*, 322, 798–807.

[5] Damghani M, Kennedy D, Featherston CA. 2011, Critical buckling of delaminated composite plates using exact stiffness analysis, *Computers and Structures*, 89, 1286-1294.

[6] Damghani M, Kennedy D, Featherston CA. 2014, Global buckling of composite plates containing rectangular delaminations using exact stiffness analysis and smearing method, *Computers and Structures*, 134, 32-47.

[7] Rock T, Hinton E. 1974 Free vibration and transient response of thick and thin plates using the finite element method. *Earthquake Engineering and Structural Dynamics*, 1974. 3: p. 51-63.

[8] Chang CN, Chiang, FK. 1988 Vibration analysis of a thick plate with an interior cut-out by a finite element method.*Journal of Sound and Vibration,* 125(3): p. 477-486.

[9] Jenq ST, Hwang GC, Yang SM. 1993 The effect of square cut-outs on the natural frequencies and mode shapes of GRP cross-ply laminates. *Composites Science and Technology*, 1993. 47(1): p. 91-101.

[10] Ju F, Lee HP, Lee KH. 1995 Free vibration of composite plates with delaminations around cutouts. *Composite Structures*, 31(2): p. 177-183.

[11] Boay CG. 1996 Free vibration of laminated composite plates with a central circular hole. *Composite Structures*, 35(4): p. 357-368.

[12] Sabir AB, Davies GT. 1997 Natural frequencies of square plates with reinforced central holes subjected to inplane loads. *Thin-Walled Structures*, 28(3-4): p. 337–353.

[13] Sabir AB, Davies GT. 1997 Natural frequencies of plates with square holes when subjected to in-plane uniaxial, biaxial or shear loading. *Thin-Walled Structures*, 28(3-4): p. 321-335.

[14] Lin CC, CS. 1998 Tseng, free vibration of polar orthotropic laminated circular and annular plates. *Journal of Sound and Vibration*, 209(5): p. 797-810.

[15] Topal U, Uzman Ü. 2008 Frequency optimization of laminated composite angle-ply plates with circular hole. *Materials & Design*, 2008. 29(8): p. 1512-1517.

[16] Dey S, Karmakar A. 2012 Free vibration analyses of multiple delaminated angle-ply composite conical shells – A finite element approach. *Composite Structures,* 94(7): p. 2188-2196.

[17] Takahashi S, 1958 Vibration of Rectangular Plates with Circular Holes. *Bulletin of JSME*, 1(4): p. 380-385.

[18] Grossi RO, Arenas BDV, Laura PAA. 1997 Free vibration of rectangular plates with circular openings. *Ocean Engineering*, 24(1): p. 19-24.

[19] Yuan J, Dickinson SM. 1996 On the vibration of annular, circular and sectorial plates with cut-outs or on partial supports. *Computers & Structures*, 58(6): p. 1261-1264.

[20] Gould SH. 1966 *Variational methods for eigenvalues problems.* London: Oxford University Press.

[21] Rayleigh JWS. 1894 The theory of sound, 2nd revised edn. New York: Dover (reprint 1945). vol. 1, pp. 110-126

[22] Ritz W. 1908 Über eine neue Methode zur Lösung gewisser Variationsprobleme der Mathematischen Physik. J. Reine Angew. Math. 135, pp 1–61.

[23] Kwak MK, Han S. 2007 Free vibration analysis of rectangular plate with a hole by means of independent coordinate coupling method, *Journal of Sound and Vibration,* 306, 12-30

[24] Wagner A, Spelsberg-Korspeter G. 2013,An efficient approach for the assembly of mass and stiffness matrices of structures with modifications, *Journal of Sound and Vibration,* 332, 4296-4307.

[25] Courant R. 1943 Variational methods for the solution of problems of equilibrium and vibration. *Bulletin of the American Mathematical Society,* 49, 1-23.

[26] Zienkiewicz OC. 1974 Constrained variational principles and penalty function methods in the finite element analysis. Lecture notes in mathematics, vol. 363, pp. 207–214. Berlin: Springer

[27] Budiansky B, Hu PC. 1946 The Lagrangian multiplier method of finding upper and lower limits to critical stresses of clamped plates, NACA report 848.

[28] Ilanko S. 2009 Embedding Negative Structures to Model Holes and Cut-Outs, *Proceedings of the 7th International Symposium on Vibrations of Continuous Systems*, 30-33, July Zakopane, Poland.

[29] Ilanko S. 2002 Existence of natural frequencies of systems with imaginary restraints and their convergence in asymptotic modelling, *Journal of Sound and Vibration*, 255, 5, 883-898

[30] Howson WP, Banerjee JR, Williams FW. 1983 Concise equations and program for exact eigensolutions of plane frames including member shear, *Advances in Engineering Software*, 5, 3, 137-141

[31] Ilanko S, Monterrubio L, Mochida Y. 2014 *The Rayleigh-Ritz Method for Structural Analysis*, pp 81-17 & 104-11, Wiley.

[32] Monterrubio LE, Ilanko S. 2015 Proof of convergence for a set of admissible functions for the Rayleigh–Ritz analysis of beams and plates and shells of rectangular planform, *Computers and Structures*, 147, 236-243.

[33] Monterrubio LE. 2009 Free vibration of shallow shells using the Rayleigh-Ritz method and penalty parameters, *Proceedings of the Institution of Mechanical Engineers, Part C: Journal of Mechanical Engineering Science*, 223, 2263-2272

[34] Ghali A, Neville AM, Cheung YK. 1972 *Structural Analysis, a unified classical and matrix approach (2nd Edition)*, London: Chapman and Hall Ltd.

[35] Zienkiewicz OC, 1977 *The Finite Element Method (3rd Edition)*, London: McGraw-Hill Book Company (UK) Limited.

[36] Petyt M, 2010 *Introduction to Finite Element Vibration Analysis (2nd Edition)*, Cambridge: Cambridge University Press

[37] Nagino H, Mikami T, Mizusawa T 2008, Three-dimensional free vibration analysis of isotropic rectangular plates using the B-spline Ritz method, *Journal of Sound and Vibration*, 317, 329-353

[38] Mochida Y, Ilanko S, 2014 Free vibration analysis of a plate with a hole using a negative plate, Proceedings of the 12th International Conference on Computational Structures Technology, Naples, Italy.

Appendix A. Dynamic Stiffness Matrix of a Three Part Beam with Clamped Ends

Consider a beam which has three segments, each of length of l_i ($i = 1,2,3$). The beam has total length L, Young's modulus E, second moment of area I and mass per unit length ρ, as shown in Fig. A1. There are four degree of freedoms numbered as shown in the figure. The natural frequencies of the beam can be found by searching frequencies ω, that satisfy Eq. (A1). The dynamic stiffness matrix ($\mathbf{K}^*$) is given as follows.
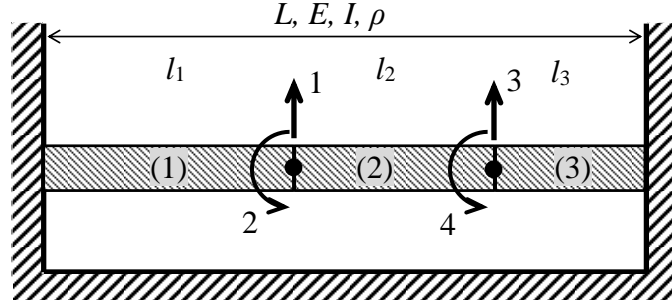

Fig. A1. A clamped-clamped beam with three segments.

$$\mathbf{K}^*\mathbf{d} = \mathbf{0} \tag{A1a}$$

$$\mathbf{K}^* = \begin{pmatrix} K_{1,1} & K_{1,2} & K_{1,3} & K_{1,4} \\ & K_{2,2} & K_{2,3} & K_{2,4} \\ & & K_{1,1} & K_{1,1} \\ Sym & & & K_{1,1} \end{pmatrix} \qquad \mathbf{d} = \begin{pmatrix} v_1 \\ \theta_2 \\ v_3 \\ \theta_4 \end{pmatrix} \tag{A1b}$$

where

$$K_{1,1} = \left(\frac{EI}{l_1^3}\right)T_{(1)} + \left(\frac{EI}{l_2^3}\right)T_{(2)} \qquad K_{1,2} = -\left(\frac{EI}{l_1^2}\right)Q_{(1)} + \left(\frac{EI}{l_2^2}\right)Q_{(2)}$$

$$K_{1,3} = -\left(\frac{EI}{l_2^3}\right)T_{(2)}t_{(2)} \qquad K_{1,4} = \left(\frac{EI}{l_2^2}\right)Q_{(2)}q_{(2)}$$

$$K_{2,2} = \left(\frac{EI}{l_1}\right)S_{(1)} + \left(\frac{EI}{l_2}\right)S_{(2)} \qquad K_{2,3} = -\left(\frac{EI}{l_2^2}\right)Q_{(2)}q_{(2)}$$

$$K_{2,4} = \left(\frac{EI}{l_2}\right)S_{(2)}C_{(2)} \qquad K_{3,3} = \left(\frac{EI}{l_2^3}\right)T_{(2)} + \left(\frac{EI}{l_3^3}\right)T_{(3)}$$

$$K_{3,4} = -\left(\frac{EI}{l_2^2}\right)Q_{(2)} + \left(\frac{EI}{l_3^2}\right)Q_{(3)} \qquad K_{4,4} = \left(\frac{EI}{l_2}\right)S_{(2)} + \left(\frac{EI}{l_3}\right)S_{(3)}$$

with

$$S_{(i)} = \lambda_{(i)}\left(\cosh \lambda_{(i)} \sin \lambda_{(i)} - \sinh \lambda_{(i)} \cos \lambda_{(i)}\right)/\left(1 - \cosh \lambda_{(i)} \cos \lambda_{(i)}\right)$$

$$C_{(i)} = \left(\sinh \lambda_{(i)} - \sin \lambda_{(i)}\right)/\left(\cosh \lambda_{(i)} \sin \lambda_{(i)} - \sinh \lambda_{(i)} \cos \lambda_{(i)}\right)$$

$$Q_{(i)} = \lambda_{(i)}^{2}\left(\sinh \lambda_{(i)} \sin \lambda_{(i)}\right)/\left(1 - \cosh \lambda_{(i)} \cos \lambda_{(i)}\right)$$

$$q_{(i)} = \left(\cosh \lambda_{(i)} - \cos \lambda_{(i)}\right)/\left(\sinh \lambda_{(i)} \sin \lambda_{(i)}\right)$$

$$T_{(i)} = \lambda_{(i)}^{3}\left(\sinh \lambda_{(i)} \cos \lambda_{(i)} + \cosh \lambda_{(i)} \sin \lambda_{(i)}\right)/\left(1 - \cosh \lambda_{(i)} \cos \lambda_{(i)}\right)$$

$$t_{(i)} = \left(\sinh \lambda_{(i)} - \sin \lambda_{(i)}\right)/\left(\sinh \lambda_{(i)} \cos \lambda_{(i)} + \cosh \lambda_{(i)} \sin \lambda_{(i)}\right)$$

and

$$\lambda_{(i)} = l_i \sqrt[4]{\omega^2 \rho/EI} \qquad (i = 1,2,3)$$

Appendix B

B.1 Rayleigh – Ritz Method

The positive plate has completely free edges and the out-plane displacement w is defined by the following admissible functions [33].

$$w(x, y, t) = W(x, y) \sin \omega t \tag{B1}$$

with

$$W(x, y) = \sum_{i=1}^{N_R} \sum_{j=1}^{N_R} G_{ij}\phi_i(x)\phi_j(y) \tag{B2}$$

and

$$\phi_i(x) = \left(\frac{x}{a}\right)^{i-1} \qquad \text{for } i = 1,2 \text{ and } 3$$

$$\phi_i(\xi) = \cos\left(\frac{(i-3)\pi x}{a}\right) \qquad \text{for } i \geq 4$$

where ω is the circular frequency and t is time. $G_{i,j}$ are undetermined weighting coefficients. The above equations are substituted into the strain energy expression, V_{max} and kinetic energy expression, T_{max} given by Eqs (B3) and (B4) respectively to obtain the stiffness matrix and mass matrix used in the Rayleigh – Ritz analysis.

$$V_{max} = \frac{1}{2}D\int_0^a \int_0^b \left[\left(\frac{\partial^2 W}{\partial x^2}\right)^2 + \left(\frac{\partial^2 W}{\partial y^2}\right)^2 + 2v\frac{\partial^2 W}{\partial x^2}\frac{\partial^2 W}{\partial y^2} + 2(1-v)\left(\frac{\partial^2 W}{\partial x \partial y}\right)^2\right] dxdy \tag{B3}$$

and

$$T_{max} = \frac{\omega^2 \rho h}{2}\int_0^a \int_0^b W^2 \, dxdy \tag{B4}$$

where

$$D = \frac{Eh^3}{12(1 - v^2)}$$

E is Young's modulus, v is Poisson's ratio, ρ is the density of the material and h is the thickness of the plate.

B.2 Finite Element Method

The hollow part is represented by the addition of the negative plate which is divided into a finite number of rectangular elements which have four nodes and 12 associated degrees of freedom, see Fig. B1. One can use the same energy expressions as in Eqs (B3) and (B4) to develop the stiffness and mass matrices using the Finite Element Method. However, the energy functional must have a minus sign as the negative plate has negative elastic modulus and negative density whose magnitudes are the same as its positive counterpart. The element stiffness and mass matrices used are given below, which are developed referring to [34-36]. For the rectangular element used in the present study, the eigenvalue equation given in Eq. (B5) is satisfied.
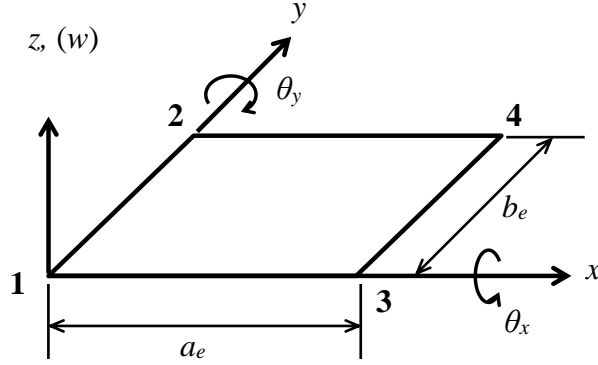

Fig. B1. A rectangular element

$$\{[K_e] - \omega^2[M_e]\}\{d\} = \{0\} \tag{B5}$$

$$\{d\} = \{d_1 \quad d_2 \quad d_3 \quad d_4\}^T \qquad \text{and} \qquad \{d_i\} = \{w_i \quad \theta_{x,i} \quad \theta_{y,i}\}^T$$

$[K_e]$ and $[M_e]$ are the element stiffness and mass matrices respectively. $\{d\}$ is the displacement vector including transverse displacement and rotations about the x and y axes.

The element stiffness matrix is given as follows.

$$[K_e] = \frac{D}{15a_e b_e} [T][S][T] \tag{B6}$$

where,

$$[S] = \begin{bmatrix}
s_{1,1} & & & & & & & & & & & \\
s_{2,1} & s_{2,2} & & & & & & & & & & \\
s_{3,1} & s_{3,2} & s_{3,3} & & & & & & \text{Sym} & & & \\
s_{4,1} & s_{4,2} & s_{4,3} & s_{4,4} & & & & & & & & \\
s_{5,1} & s_{5,2} & s_{5,3} & s_{5,4} & s_{5,5} & & & & & & & \\
s_{6,1} & s_{6,2} & s_{6,3} & s_{6,4} & s_{6,5} & s_{6,6} & & & & & & \\
s_{7,1} & s_{7,2} & s_{7,3} & s_{7,4} & s_{7,5} & s_{7,6} & s_{7,7} & & & & & \\
s_{8,1} & s_{8,2} & s_{8,3} & s_{8,4} & s_{8,5} & s_{8,6} & s_{8,7} & s_{8,8} & & & & \\
s_{9,1} & s_{9,2} & s_{9,3} & s_{9,4} & s_{9,5} & s_{9,6} & s_{9,7} & s_{9,8} & s_{9,9} & & & \\
s_{10,1} & s_{10,2} & s_{10,3} & s_{10,4} & s_{10,5} & s_{10,6} & s_{10,7} & s_{10,8} & s_{10,9} & s_{10,10} & & \\
s_{11,1} & s_{11,2} & s_{11,3} & s_{11,4} & s_{11,5} & s_{11,6} & s_{11,7} & s_{11,8} & s_{11,9} & s_{11,10} & s_{11,11} & \\
s_{12,1} & s_{12,2} & s_{12,3} & s_{12,4} & s_{12,5} & s_{12,6} & s_{12,7} & s_{12,8} & s_{12,9} & s_{12,10} & s_{12,11} & s_{12,12}
\end{bmatrix}$$

with

$s_{1,1} = 60(\beta^2 + \alpha^2) - 12\nu + 42$

$s_{2,1} = 30\alpha^2 + 12\nu + 3, \qquad s_{2,2} = 20\alpha^2 - 4\nu + 4,$

$s_{3,1} = -(30\beta^2 + 12\nu + 3), \quad s_{3,2} = -15\nu, \qquad s_{3,3} = 20\beta^2 - 4\nu + 4,$

$s_{4,1} = 30(\beta^2 - 2\alpha^2) + 12\nu - 42, \qquad s_{4,2} = -30\alpha^2 + 3\nu - 3,$

$s_{4,3} = -15\beta^2 + 12\nu + 3, \qquad s_{4,4} = 60(\beta^2 + \alpha^2) - 12\nu + 42$

$s_{5,1} = 30\alpha^2 + 12\nu + 3, \qquad s_{5,2} = 10\alpha^2 + \nu - 1, \qquad s_{5,3} = 0,$

$s_{5,4} = -(30\alpha^2 + 12\nu + 3), \qquad s_{5,5} = 20\alpha^2 - 4\nu + 4,$

$s_{6,1} = -15\beta^2 + 12\nu + 3, \qquad s_{6,2} = 0, \qquad s_{6,3} = 10\beta^2 + 4\nu - 4, \qquad s_{6,4} = -(30\beta^2 + 12\nu + 3),$

$s_{6,5} = 15\nu, \quad s_{6,6} = 20\beta^2 - 4\nu + 4,$

$s_{7,1} = 30(-2\beta^2 + \alpha^2) + 12\nu - 42, \qquad s_{7,2} = 15\alpha^2 - 12\nu - 3,$

$s_{7,3} = 30\beta^2 - 3\nu + 3, \qquad s_{7,4} = -30(\beta^2 + \alpha^2) - 12\nu + 42, \qquad s_{7,5} = 15\alpha^2 + 3\nu - 3,$

$s_{7,6} = 15\beta^2 + 3\nu - 3, \quad s_{7,7} = 60(\beta^2 + \alpha^2) - 12\nu + 42$

$s_{8,1} = 15\alpha^2 - 12\nu - 3, \qquad s_{8,2} = 10\alpha^2 + 4\nu - 4, \qquad s_{8,3} = 0, \qquad s_{8,4} = -15\alpha^2 - 3\nu + 3,$

$s_{8,5} = 5\alpha^2 - \nu + 1, \qquad s_{8,6} = 0, \qquad s_{8,7} = 30\alpha^2 + 12\nu + 3, \qquad s_{8,8} = 20\alpha^2 - 4\nu + 4,$

$s_{9,1} = -30\beta^2 + 3\nu - 3, \qquad s_{9,2} = 0, \qquad s_{9,3} = 10\beta^2 + \nu - 1, \qquad s_{9,4} = -15\beta^2 - 3\nu + 3,$

$s_{9,5} = 0, \qquad s_{9,6} = 5\beta^2 - \nu + 1, \qquad s_{9,7} = 30\beta^2 + 12\nu + 3, \qquad s_{9,8} = 15\nu, \qquad s_{9,9} = 20\beta^2 - 4\nu + 4$

$s_{10,1} = -30(\beta^2 + \alpha^2) - 12\nu + 42, \qquad s_{10,2} = -15\alpha^2 - 3\nu - 3, \qquad s_{10,3} = 15\beta^2 + 3\nu - 3,$

$s_{10,4} = 30(-2\beta^2 + \alpha^2) + 12\nu - 42, \qquad s_{10,5} = -15\alpha^2 + 12\nu + 3, \qquad s_{10,6} = 30\beta^2 - 3\nu + 3,$

$s_{10,7} = 30(\beta^2 - 2\alpha^2) + 12\nu - 42, \qquad s_{10,8} = -30(\beta^2 + \alpha^2) - 12\nu + 42,$

$\qquad s_{10,9} = 15\beta^2 - 12\nu - 3,$

$s_{10,10} = 60(\beta^2 + \alpha^2) - 12\nu + 42$

$s_{11,1} = 15\alpha^2 + 3\nu - 3, \qquad s_{11,2} = 5\alpha^2 - \nu + 1, \qquad s_{11,3} = 0, \qquad s_{11,4} = -15\alpha^2 + 12\nu + 3,$

$s_{11,5} = 10\alpha^2 + 4\nu - 4, \qquad s_{11,6} = 0, \qquad s_{11,7} = 30\alpha^2 - 3\nu + 3, \qquad s_{11,8} = 10\alpha^2 + \nu - 1,$

$s_{11,9} = 0, \qquad s_{11,4} = -(30\alpha^2 + 12\nu + 3), \qquad s_{11,5} = 20\alpha^2 - 4\nu + 4$

$s_{12,1} = -15\beta^2 - 3\nu + 3, \qquad s_{12,2} = 0, \qquad s_{9,3} = 5\beta^2 - \nu + 1, \qquad s_{12,4} = -30\beta^2 + 3\nu - 3,$

$s_{12,5} = 0, \qquad s_{12,6} = 10\beta^2 + \nu - 1, \qquad s_{12,7} = 15\beta^2 - 12\nu - 3, \qquad s_{12,8} = 0,$

$\qquad s_{12,9} = 10\beta^2 - 4\nu - 4,$

$$s_{12,10} = 30\beta^2 + 12\nu + 3, \qquad s_{12,11} = -15\nu, \qquad s_{12,12} = 20\beta^2 - 4\nu + 4$$

$$(\alpha = a_e/b_e, \qquad \beta = b_e/a_e)$$

and

$$[T] = \begin{bmatrix} l & & \\ & l & \\ & & l \end{bmatrix} \qquad \text{and} \qquad [l] = \begin{bmatrix} 1 & & \\ & a_e & \\ & & b_e \end{bmatrix}$$

The element mass matrix is given in the following form.

$$[M_e] = \frac{\rho a_e b_e}{25200} \begin{bmatrix} \mathbf{m}_{11} & \mathbf{m}_{21}^{\mathrm{T}} \\ \mathbf{m}_{21} & \mathbf{m}_{22} \end{bmatrix} \tag{B7}$$

where

$$\mathbf{m}_{11} = \begin{bmatrix} 3454 & & & & & \\ 461b_e & 80b_e^2 & & & \text{Sym} & \\ -461a_e & -63a_eb_e & 80a_e^2 & & & \\ 1226 & 274b_e & -199a_e & 3454 & & \\ 274b_e & -60b_e^2 & 42a_eb_e & -461b_e & 80b_e^2 & \\ -199a_e & -42a_eb_e & 40a_e^2 & -461a_e & 63a_eb_e & 80a_e^2 \end{bmatrix}$$

$$\mathbf{m}_{21} = \begin{bmatrix} 1226 & 199b_e & -274a_e & 394 & -116b_e & -116a_e \\ 199b_e & 40b_e^2 & -42a_eb_e & 116b_e & -30b_e^2 & -28a_eb_e \\ 274a_e & 42a_eb_e & -60a_e^2 & 116a_e & -28a_eb_e & -30a_e^2 \\ 394 & 116b_e & -116a_e & 1226 & -199b_e & -274a_e \\ -116b_e & -30b_e^2 & 28a_eb_e & -199b_e & 40b_e^2 & 42a_eb_e \\ 116a_e & 28a_eb_e & -30a_e^2 & 274a_e & -42a_eb_e & -60a_e^2 \end{bmatrix}$$

$$\mathbf{m}_{22} = \begin{bmatrix} 3454 & & & & & \\ 461b_e & 80b_e^2 & & & \text{Sym} & \\ 461a_e & 63a_eb_e & 80a_e^2 & & & \\ 1226 & 274b_e & 199a_e & 3454 & & \\ -274b_e & -60b_e^2 & -42a_eb_e & -461b_e & 80b_e^2 & \\ 199a_e & 42a_eb_e & 40a_e^2 & 461a_e & -63a_eb_e & 80a_e^2 \end{bmatrix}$$

B.3 Penalty Method

The continuity conditions between the two plates are satisfied asymptotically by inserting artificial springs with very high stiffness between them and adding the potential energy due to the springs as penalty terms to the Rayleigh-Ritz minimisation equations. Using the notation in reference [37] the potential energy, L_{max} is given by the following equations.

$$L_{max} = \frac{1}{2} \sum_{i}^{N_h} \sum_{j}^{N_h} k_w \left\{ W(x_i, y_j) - d_{h_{i,j}} \right\}^2 \tag{B8}$$

N_h is the number of the finite element nodes in the x and y directions for the hollow part, and x_i and y_j are the coordinates of the positive plate corresponding to the nodes. $d_{hi,j}$ is the transverse displacement of the negative plate at the nodes and k_w is the penalty parameter. For this study, the value of k_w was chosen as 10^{10} times the plate flexural rigidity, D (i.e. $k_w = 10^{10}D$) since the value is sufficient to be considered as an asymptotically rigid connection from the results in [38].

B.4 Eigenmatrix Equation

The total energy functional, $(V_{max} + L_{max}) - T_{max}$ is minimised with respect to the unknown weighting coefficients and nodal degrees of freedom using the Rayleigh – Ritz procedure which yields an eigenvalue equation

$$\{[K] - \omega^2 [M]\} \begin{Bmatrix} G \\ d_h \end{Bmatrix} = \{0\} \tag{B9}$$

in which

$$[K] = \begin{bmatrix} K_{pos} + K_p & -K_{ph}^T \\ -K_{ph} & K_{neg} + K_{phh} \end{bmatrix}, \qquad [M] = \begin{bmatrix} M_{pos} & 0 \\ 0 & M_{neg} \end{bmatrix}$$

where $[K]$ and $[M]$ are stiffness and mass matrices, and the subscripts *pos* and *neg* stand for the positive and negative structure respectively. $[K_p]$ are stiffness sub-matrices due to the penalty terms. $\{G\}^T$ and $\{d_h\}^T$ are sets of coefficient vectors for the positive plate and degrees of freedom of the negative plate respectively. The non-dimensional frequency parameters, $\Omega = \omega a^2 \sqrt{\rho h / D}$ are obtained by solving the above eigenvalue equation.